PROCEEDINGS OF THE 9th SYMPOSIUM ON THE GEOLOGY OF THE BAHAMAS AND OTHER CARBONATE REGIONS

Edited by
H. Allen Curran and John E. Mylroie

Production Editors:
Matthew A. Reece
Laurel L. Powers

Bahamian Field Station, Ltd.
San Salvador, Bahamas
1999

Front Cover: Lee-side exposure of a fossil parabolic dune viewed from the Grahams Harbour side (west) of North Point, San Salvador, Bahamas. These Holocene carbonate eolianites have been assigned to the North Point Member of the Rice Bay Formation (Carew and Mylroie, 1995). The eolian cross-stratification dips below present sea level, proving that late Holocene sea-level rise is real. Top of the dune is about 7 meters above the sea surface. Photo by Al Curran.

Back Cover: Dr. Noel P. James of Queen's University, Kingston, Ontario, Canada, keynote speaker for this symposium. Noel is holding a carving of a tropical fish created by a local artist and presented to him at the end of the symposium. Photo by Al Curran.

Printed in USA by

ISBN 0-935909-67-2

MODELING THE FRESH WATER - SALT WATER INTERFACE IN THE PLEISTOCENE AQUIFER ON ANDROS ISLAND, BAHAMAS

John M. Bukowski
Lockheed Martin Idaho Technologies Co.
Idaho National Engineering and Environmental Laboratory
P.O. Box 1625, M.S. 3953
Idaho Falls, ID 83415-3953

Cindy Carney
Department of Geological Sciences
Wright State University
Dayton, OH 45435

Robert W. Ritzi, Jr.
Department of Geological Sciences
Wright State University
Dayton, OH 45435

Mark R. Boardman
Department of Geology
Miami University
Oxford, OH 45056

ABSTRACT

The fresh water lens in the Pleistocene carbonate aquifer on Andros Island, Bahamas is significantly thinner than the Ghyben-Herzberg (GH) theoretical lens, with depth below sea level approximately 10 times the head above sea level as opposed to 40 times. Factors that may affect lens thickness but are not considered by Ghyben-Herzberg theory include variable lithology, recharge, and the subsequent flow and transport processes. These factors were considered in this study by using a numerical model for density dependent ground water flow and salt transport in order to explore the sensitivity of lens thickness to the factors. The model represented a two dimensional vertical cross section of Andros Island and included parameters based both on existing data and new data collected from field investigations.

The simulations were appreciably sensitive only to variations in lithology. Simulations that represented the discrete intervals of low-permeability paleosols which occur on Andros resulted in salinity profiles and a lens thickness similar to conditions observed on the island. Simulations were also run using layered heterogeneity, along with anisotropy values estimated from field pumping test data. In these models, aquifer permeability in the vertical direction was three orders of magnitude greater than horizontal permeability, however because of paleosols, the harmonic average of vertical permeability across layers remained the same as in the isotropic models, and lens thickness did not significantly change. Thus heterogeneity across layers, not anisotropy within layers, can explain the thinness of the lens on Andros.

Paleosols also exist beneath the other northwestern Bahamian island and at similar depth to those on Andros. The lenses on these other islands are also thinner than the GH theo-

retical lens and are consistent with the results of this study.

INTRODUCTION

Fresh water lenses on the Bahamian Islands are significantly thinner than would be predicted by the Ghyben-Herzberg principle (Fetter, 1972; Little et al., 1973; Cant and Weech, 1986; Lloyd, 1991; Vacher and Wallis, 1992; Wolfe et al., 1995; Bukowski, 1996). Ignoring anthropogenic influences, the size and shape of the fresh water lenses can be controlled by recharge, lithology, ground-water flow, and salt transport between fresh and sea water (Cant and Weech, 1986; Underwood et al., 1992; Vacher and Wallis, 1992).

The primary goal of this study was to provide a better understanding of the factors that control the thickness of the naturally occurring fresh water lens on Andros Island, the largest of the Bahamian Islands (Figure 1). The objective was to develop an interpretive numerical model for the Pleistocene carbonate aquifer. Parameters for the numerical model were based on a combination of existing data and new data collected at a field site located on north Andros Island (Figure 2). The model parameters representing the factors were varied in a sensitivity analysis in order to understand which factors most strongly influence and therefore do indeed control the thickness of the fresh water lens.

Understanding the fresh water lens thickness is important for effectively managing it as a resource. New Providence Island, located 45 km east of Andros, currently receives several million gallons per day of fresh water exported from wellfields in the northern region of Andros. The daily export of fresh water is estimated to meet over 50% of the drinking water demand in Nassau, New Providence. Data from pumping centers maintained by the Water and Sewerage Corporation indicate that annual yields are significantly exceeding design capacities. Withdrawal for potable water has caused depletion of aquifer storage resulting in thinning of the

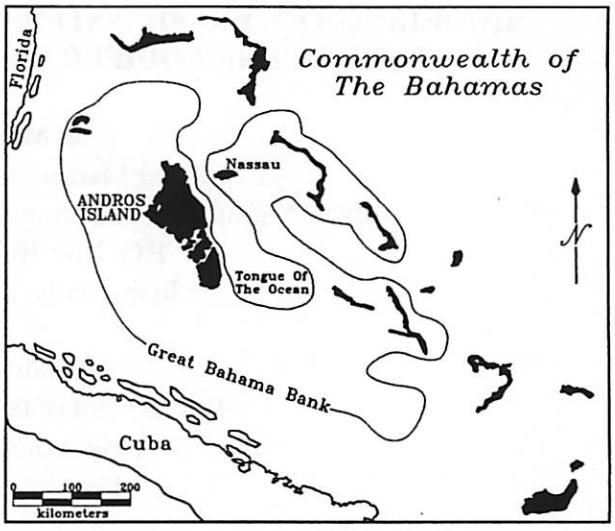

Figure 1. Map of Bahamas and location of Andros Island.

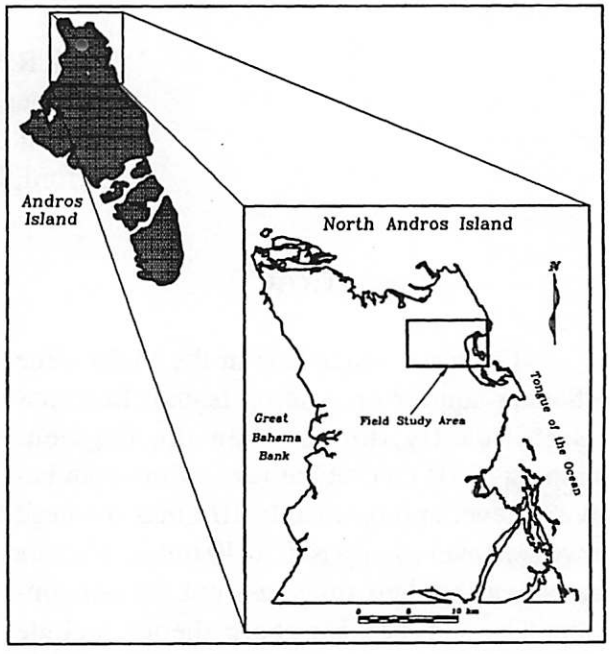

Figure 2. Field study area on north Andros Island.

fresh water lens and upconing of salt water (Weech, 1995, personal communication). Continued over-abstraction will result in further salt water upconing and diminish the value of Andros as a source of fresh water. Understanding the natural controls on fresh water lens thickness is an important first step toward building future

models representing the ground water flow system, including local scale models specifically representing abstraction by the wellfields.

INVESTIGATIONS OF THE FRESH WATER LENS

During 1971 and 1972 a survey was conducted by the British Government to evaluate the land resources of Andros Island (Little et al., 1973) including the island's aquifer system. They sought to define the boundaries of the fresh water lens and to formulate pumping rates which would enable development on the island to proceed without over-abstraction.

During the time of the survey, 120 percussion boreholes and three cored holes were drilled ranging in depth from 1.5 to 40 m, for the purpose of estimating the thickness of the fresh water lens. While drilling, the ground water was depth-sampled at 1.5 m intervals and analyzed for chloride content. The drilling stopped when the chloride content reached or exceeded 500 ppm. Data collected from this investigation were used to conceptualize the position of the fresh water - salt water interface in Figure 3. It is inferred that the thickest portion of potable water (chloride concentration ≥500 ppm) is about 15 m and thins to zero at the ocean.

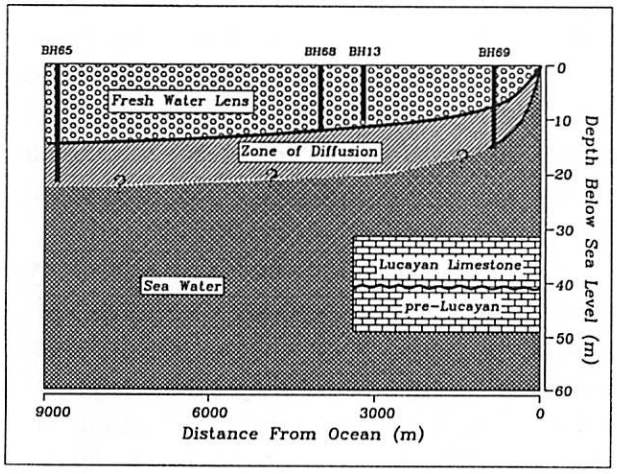

Figure 3. Conceptual model of fresh water - salt water interface constructed from data by Little et al. (1973).

This thickness (15m) is significantly less than the theoretical Ghyben Herzberg (GH) lens, i.e. the depth below sea level is currently approximately 10 times the head above sea level, and the GH model predicts the head above sea level to be 40 times.

Other studies are consistent with this conceptual model (Little et al., 1973; Peach, 1991; Wolfe et al., 1995; Boardman and Carney, 1997). Resistivity soundings in the vicinity of several shallow boreholes (maximum depth 12.5 m) drilled by Boardman and Carney (1997) and a blue hole in the study area produced results which indicated the fresh water lens begins at 1.2 m to 1.5 m a.s.l. and ranges in thickness from 5.3 to 13.3 m (Wolfe et al., 1995). As ground-truth support for the surveys, we measured the base of the fresh water lens in a nearby borehole, and this measurement confirmed the position of the base of the lens estimated by the resistivity studies. Peach (1991) estimated the depth to the fresh water - salt water interface on north Andros Island from Offset-Wenner resistivity soundings. Models produced from the data estimate that the thickest part of the lens in the area of the northern Andros Island wellfields is about 17 m.

The conceptual model conveyed in Figure 3, developed from Little et al. (1973) seems to be consistent with the thin lens implied in the results of all these other studies. Thus, the results from numerical simulations will be compared to this conceptualization of the lens and diffusion zone.

CONTROLS ON THE THICKNESS OF THE FRESH WATER LENS

Recharge

Recharge to the fresh water lens is equal to precipitation minus losses due to evaporation, transpiration, and surface runoff. The average annual precipitation in the Bahamas is conveyed in the isohyetal map (Figure 4) and illustrates that precipitation generally decreases from 130

cm/year in the northwest to 75 cm/year in the southeast (Cant and Weech, 1986; Sealey, 1994). The mean of available precipitation data on north Andros is 120 cm per year. Cant and Weech (1986) have observed that Bahamian islands receiving greater than 110 cm per year have continuous, cross-island fresh water lenses, as seen on Andros, and islands receiving less than 110 cm per year have localized, discontinuous lenses. For those islands maintaining continuous lenses, such as Andros, Little et al. (1973) used available meteorological data to estimate that recharge to the aquifer is equal to 25% of precipitation or 30 cm/yr.

Topographically, the island is relatively flat and close to sea level (Boardman et al., 1992). Tidal flat areas on the western margin of the island are generally less than 0.5 m above

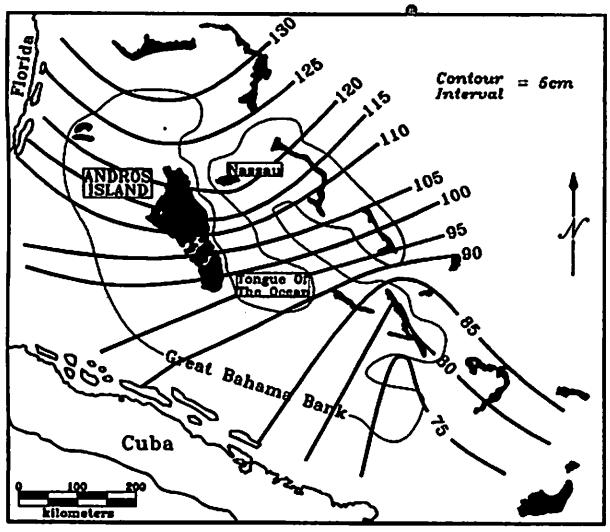

Figure 4. Isohyetal map of average annual precipitation in the Bahamas (modified from Cant and Weech, 1986; Cowles, 1993; Sealey, 1994).

sea level. Flat lands further to the north and east do not exceed 5 m in elevation. Dune ridges comprised of Pleistocene rock represent the greatest relief on the island and are only a few meters higher than the adjacent land surface. The relatively flat topography may affect the elevation at which recharge occurs, and even the low relief can significantly affect the hydraulic gradient controlling ground water flow.

Lithology

Changes in subsurface lithology may affect lens thickness in that lithologic changes may create changes in the hydraulic properties of the subsurface, including permeability, storage, and dispersivity. These hydraulic properties are discussed in the next section on flow and transport.

The Great Bahama Bank is a low platform of the Pleistocene Lucayan Limestone (Beach and Ginsburg, 1980). Two major facies within the Lucayan are lagoonal and eolian dune deposits which form low arcuate dune ridges (Shinn and Lidz, 1988). Beach and Ginsburg (1980) estimate that the average thickness of the formation is 43 m based on several cores drilled on the northwestern Bahama Bank.

On Andros, the stratigraphy in the upper 25 m of the Lucayan Limestone in the study area is depicted in Figure 5. The upper 2 m is laminated, oolitic and peloidal grainstones (Boardman et al., 1992). The zone from 2 to 10 m is burrowed oolitic grainstones and packstones (Carney and Boardman, 1993). From 10 to 15 m below surface, the lithology has been characterized as a highly burrowed wackestone. Porosity in the upper 15 m increases with depth and ranges from 10 to 20% (Boardman and Carney, 1997). Below 15 m, the rock is crystalline oolitic limestone with fossils represented by molds and burrow walls preserved. A marked increase in porosity has been observed, though not specifically quantified, at 25 m (Peach, 1991).

A special situation is presented by paleosol layers. Paleosols are low permeability strata produced during subaerial exposure. Such strata is characterized by one or more of the following features: (1) dense laminated calcareous, caliche crusts; (2) red to brown leaching and staining; (3) blackened clasts; (4) narrow bands of dark gray micrite; and (5) abrupt facies changes (Beach and Ginsburg, 1980;

Shinn and Lidz, 1988; Peach, 1991; Aurell et al., 1995; Boardman et al., 1995; Kenter et al., 1995).

Core borings taken from the northwestern Bahama Bank record paleosols distributed

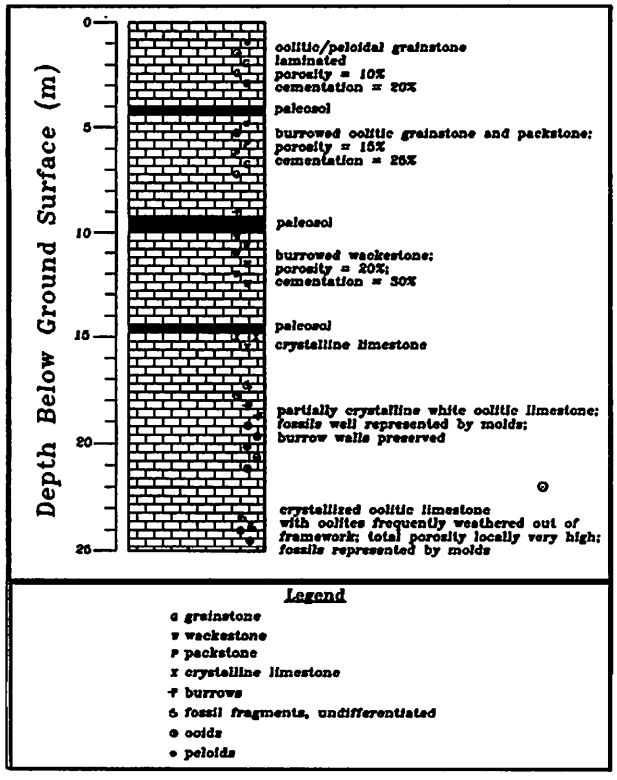

Figure 5. Lithologic description of upper 25 m of Lucayan Limestone (Peach, 1991; Boardman et al., 1992; Boardman and Carney, 1997).

throughout the Lucayan at an average of one per 3 m of core (Beach and Ginsburg, 1980). Other cores taken from the Bahama Bank have included 13 horizons of laminated crusts and blackened pebbles in the upper 100-150 m of the borings (Kenter et al., 1995). Peach (1991) indicates that caliche crusts can be up to 0.75 m thick and mark areas of low vertical permeability in the formation. Cores drilled in the north Andros study area include distinct horizons of black grains, laminated crusts, and staining characteristic of a paleosol (Boardman and Carney, 1997). The paleosol horizons from the north Andros cores range in thickness from a few decimeters to more than one meter.

Flow and Transport

Factors associated with ground water flow and solute transport include permeability, porosity, fluid density, advection, mechanical dispersion, diffusion, and tidal fluctuations. Several researchers have found that fresh water lenses in the Bahamas are thinner than what the hydrostatic GH theory predicts and thus that the lenses are likely influenced by flow and transport factors (Cant and Weech, 1986; Vacher and Wallis, 1992; Wolfe et al., 1995). Existing data and data collected from field investigations conducted in this study (Little et al., 1973; Bukowski, 1996) associated with permeability are presented in Tables 1 and 2.

The Dupuit-Ghyben-Herzberg analytical model for coastal aquifers accounts for recharge and one-dimensional flow to compute an estimate of fresh water head:

$$h^2 = \frac{W\left[a^2 - (a-x)^2\right]}{K(1+G)} \qquad (1)$$

where: h = elevation of water table (L);
W = recharge rate (L/T);
a = half width of island (L);
K = hydraulic conductivity (L/T);

$$G = \frac{\rho_f}{\rho_s - \rho_f} = \frac{1}{1.025 - 1.0} = 40$$

r_f = density of fresh water (M/L^3);
r_s = density of salt water (M/L^3);

and the GH principle to compute lens thickness. The water table elevation will be lower, and thus the lens will be thinner if W is lower and K greater. A recharge value of 11 cm/yr would be 10% of average annual precipitation and at the lower end of the range of reasonable values. A hydraulic conductivity of 5.0×10^{-2} cm/s represents estimates from pumping tests. With these values, the analytical solution gives a reasonable head profile but gives a fresh water lens

Hydraulic Parameters Estimated from Pumping Tests (1971-1972)

borehole	Transmissivity (cm^2/s)	Permeability (cm^2) assuming b= 5.0 m	borehole	Transmissivity (cm^2/s)	Permeability (cm^2) assuming b=5.0 m
14	1.3E+01	2.6E-07	51	2.3E+02	4.76E-06
15	3.8E+03	7.8E-05	52	4.7E+01	9.51E-07
18	2.6E+03	5.4E-05	52	9.9E+02	2.03E-05
19	5.4E+03	1.1E-04	53	4.9E+03	1.00E-04
22	2.6E+03	5.2E-05	55	3.5E+03	7.05E-05
28	4.3E+02	8.7E-06	57	3.5E+03	7.05E-05
32	6.9E+02	1.4E-05	62	1.9E+03	3.88E-05
34	1.8E+03	3.7E-05	63	1.7E+03	3.45E-05
35	1.1E+01	2.1E-07	63	3.3E+03	6.73E-05
39	2.8E+03	5.6E-05	64	9.8E+02	1.99E-05
40	1.9E+03	3.8E-05	68	2.3E+03	4.62E-05
41	3.3E+02	6.7E-06	74	2.6E+03	5.25E-05
43	3.2E+02	6.6E-06	80	2.0E+03	4.12E-05
49	2.1E+02	4.4E-06	84	1.9E+03	3.91E-05
49	2.5E+03	5.0E-05	89	3.4E+03	6.91E-05
50	1.4E+04	2.8E-04			

Hydraulic Parameters Estimated from Tidal Response (1971-1972)

borehole	Transmissivity (cm^2/s) from fluctuation ratio	Permeability (cm^2) assuming b=10 m	Transmissivity (cm^2/s) from time lag	Permeability (cm^2) assuming b=10 m
71-91-80	2.3E+06	2.4E-02	5.8E+06	6.0E-02
70-69-1-76-89	4.8E+06	4.9E-02	2.7E+06	2.8E-02
67-13-68-1-5-14	6.0E+06	6.1E-02	1.4E+07	1.5E-01
102-103-104-58	7.0E+06	7.2E-02	3.0E+07	3.0E-01
100-101-50-52-59	1.9E+07	1.9E-01	2.5E+07	2.6E-01
30-31-41	1.0E+07	1.1E-01	3.5E+07	3.6E-01
8-9-17-18	1.0E+07	1.0E-01	2.7E+07	2.8E-01
21-19-64	1.9E+07	1.9E-01	3.2E+07	3.3E-01
46-45-49-63	3.1E+07	3.2E-01	2.6E+07	2.7E-01

Table 1. Hydraulic parameters estimated from British Land Survey (1973).

Hydraulic Parameters Estimated from Tidal Response (1995)

Location	Transmissivity (cm^2/s) from attenuation	Permeability (cm^2) assuming b=10 m	Transmissivity (cm^2/s) from phase shift	Permeability (cm^2) assuming b=10 m
BH69	9.3E+01	9.5E-05	1.7E+00	1.7E-06

Hydraulic Parameters Estimated from Pumping Tests (1996)

Location	Method of Analysis	Transmissivity (cm^2/s)	Permeability (cm^2) assuming b=5.0 m
2NN	Neuman (1975) log-log	1.7E+00	k_H=3.8E-8; k_V=1.1E-4

Hydraulic Parameters Estimated from Slug Tests (1995)

Location	Hydraulic Conductivity (cm/s)	Permeability (cm^2)
4SA	4.3E-06	4.4E-11
91	4.6E-06	4.7E-11
C69	4.9E-04	5.0E-09

Table 2. Hydraulic parameters estimated from 1994, 1995, and 1996 field studies.

thickness of 150 m which is on the order of 130 m too thick (see section 2). Recharge rates and hydraulic conductivity within reasonable ranges give lens thicknesses that are also on the order of 100 m too large; a model accounting for other factors is required.

Variability in lithology gives rise to variability in hydraulic conductivity which affects flow in ways not accounted for in equation 1. Other factors can be accounted for in the diffusion and the advection-dispersion equations:

$$\frac{\partial}{\partial x_i}\frac{k_{ij}\gamma}{\mu}\frac{\partial h}{\partial x_i} = S_s\frac{\partial h}{\partial t} \pm q^* \quad (2)$$

$$\frac{\partial}{\partial x_i}\left(D_{ij}\frac{\partial}{\partial x_j}\right) - \frac{\partial}{\partial x_i}(cv_i) = R_d\frac{\partial_c}{\partial_t} + \lambda c R_d - \frac{C'W^*}{n_c} \quad i,j = x, y, z \quad (3)$$

where: h = head (L);
k = permeability (L^2);
m= viscosity (M/LT);
g= specific weight (M/L^2T^2),
S_s = specific storage (L-1);
v_i = components of the velocity vector (L/T);
D_{ij} = dispersion coefficient (L^2/T);
c = concentration (M/L);
Rd = retardation factors (dim);
l= first-order rate constant (dim);
C' = known source concentration (M/L);
W* = source/sink term of mass (M/L);
q*= source/sink fluid including recharge (L/T),

and

$$\rho(C) = \rho + \frac{\partial_\rho}{\partial_c}(C - C_o) \quad (4)$$

where: $\rho(C)$ = density of fluid at concentration C (M/L^3);
ρ_0 = density at base fresh water concentration (M/L^3);
C = concentration of fluid at a given nodal point (M/L);
C_0 = concentration of fresh water (M/L);

$\frac{\partial_\rho}{\partial_c}$ = fluid coefficient of density change with concentration (dim).

In equations 2 and 3, changes in lithology can be represented in the assignment of the hydraulic conductivity and dispersion coefficient of the porous medium. The ocean source of salt and tidal variations are represented by stating conditions on the boundary domain.

Several studies have used the numerical solutions of these equations to simulate the flow regime of coastal and small atoll island aquifers (Herman and Wheatcraft, 1984; Hogan, 1988; Oberdorfer et al., 1990; Griggs, 1989; Griggs and Peterson, 1989; Underwood, 1990; Underwood et al., 1992; Wicks and Herman, 1995). Oberdorfer et al. (1990) used a numerical model to test theories regarding the geologic control on flow patterns including the effects of tidally driven flow and found that tide-induced dispersion and horizontal mixing contribute to horizontal and vertical flow. Failure to consider these processes results in an underestimation of the mixing zone and overestimation of the fresh water lens thickness. Underwood et al. (1992) compared simulations with tidal versus non-tidal boundary conditions. Model runs simulating tidal fluctuations broadened the transition zone between fresh and salt water, and thereby thinned the fresh water lens. A one meter increase in the simulated tidal range resulted in approximately a 5.0 m thinning of the fresh water lens. However, Little et al. (1973) observed on Andros Island that in deeper blue holes (circular lakes formed by sink holes) and boreholes, which have a greater hydraulic connection with the ocean, the tidal amplitude was not related to the ratio

of thickness of the fresh water lens to head above sea level. Furthermore, the tidal amplitude from the shore inward is generally less than 1 m, and thus the relationship observed by Underwood et al. (1992) (1 m amplitude/5 m thinning) could not account for the approximately 100 m thining as compared to GH theory.

NUMERICAL MODELING

The equations for solute transport (equations 2, 3, and 4) were solved using a two-dimensional numerical approach (Voss, 1984). The grid and boundaries of the model were based on conceptualization of the aquifer as illustrated in Figure 3. The model represents a vertical cross section of the eastern half of the island. The grid was 9000 m long, representing an average distance from mid-island to ocean, and 170 m deep, a distance great enough to incorporate ocean circulation beneath the mixing zone. The western portion of the model corresponds to what is likely a drainage divide. The eastern

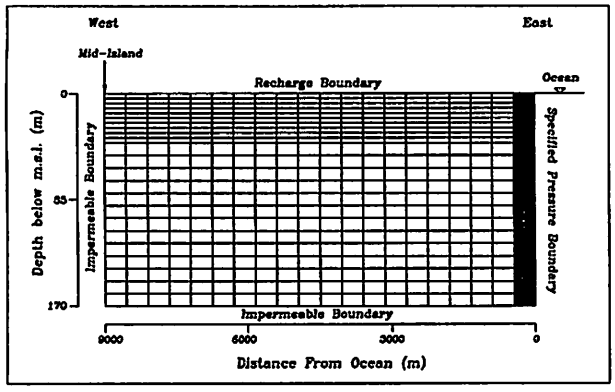

Figure 6. Two-dimensional finite element grid and boundary conditions.

vertical edge of the model is used to simulate the relatively vertical interface with the ocean along the island's eastern margin, where water depth >3000 m is found in a deep marine trough known as The Tongue of the Ocean (see Figure 1). Topographic relief was varied in the simulations but kept <2 m representing the relatively flat-lying island surface.

The initial finite element grid shown in Figure 6 was designed to be finer where the fresh water lens would likely be positioned. Likewise, the grid is finer along the right boundary to more rigorously account for hydrodynamic processes associated with flow from the ocean. This grid gives Peclet numbers that exceed 2, however, generally the simulations were generally well behaved as discussed below.

The upper boundary represented the water table (pressure = 0) under different topographic and recharge scenarios we investigated, decreasing from mid-island to zero at the ocean and was initially determined according to the Dupuit-Darcy equation. Because the eastern margin of the island has a relatively vertical interface with the ocean, pressure was prescribed based on depth below sea level. No flow boundaries were specified at the bottom of the grid and at the flow divide along the left vertical boundary. The boundary conditions for the mass transport model were specified as the concentration of sea water along the right side of the grid and zero flux for the other three boundaries. The value used for sea water concentration is the standard for the mass fraction of total dissolved solids in sea water equal to 0.0357 kg salt / kg sea water. Tidal variations were not simulated because field observations discussed previously give evidence that they do not exert a significant influence.

Although the goal of the simulations was to determine a steady state fresh water lens configuration, the transport model needed to be run transient to an equilibrated condition. A ten day time step was used, which gave Courant numbers below unity over most of the grid as recommended (Anderson and Woessner, 1992), and gave results that were the same as using 1 day time steps in comparison among early simulations.

An initial simulation consisted of a homogeneous domain where permeability in all elements was set equal to 5.1×10^{-7} cm^2, a value equal to that used in the Dupuit-Ghyben-Herzberg model and representative of results

from tidal fluctuation studies, pumping tests, and slug tests given in Tables 1 and 2 (Little et al., 1973; Bukowski, 1996). The fresh water lens from this setup resulted in a thickness that was on the order of 130 m as shown in Figure 7a. The isochlors give the mass fraction of total dissolved solids in sea water. The 0.0009 contour is equivalent to 500 ppm chlorinity and is related to salinity by the equation (Thurman, 1991):

$$\left(\text{salinity} \left(\frac{\text{kg salt}}{\text{kg seawater}} \right) / 1.80655 \right) * 1\text{x}10^{6} = \text{chlorinity (ppm)} \quad (5)$$

In a subsequent model we assigned permeability in the upper 40 m as 10^{-9} cm^2 corresponding to slug test results from the Lucayan (Little et al., 1973; Bukowski, 1996) The grid which extended from 40 to 170 m below ground surface was assigned a permeability value of 10^{-5} cm^2 corresponding to the pre-Lucayan portion, as estimated from tidal response (Little et al., 1973; Bukowski, 1996). The porosity of the sediments in the upper 40 m of the model was assigned a value 0.20 as reported by petrographic analysis of core samples (Boardman and Carney, 1997). A porosity of 0.35 was used in the lower, more permeable zone based on marked increases in porosity observed by several researchers (e.g., Little et al., 1973; Beach and Ginsburg, 1980; Peach, 1991). Dispersivity has not been measured. The longitudinal value used was 1.0 m and the transverse value was 0.1 m. To evaluate sensitivity, these values were varied in numerous simulations and only unreasonably large dispersivities, beyond 100 m for the limestone aquifer, affected the results. Results from the setup had a fresh water lens 70 m thick as shown in Figure 7b.

To the previous model, a paleosol was added in the Lucayan Limestone by specifying a permeability value of 10^{-16} cm^2 to layer 2 (4 m thick) of the grid. As shown in Figure 7c, the fresh water lens thins considerably to 25 m and more closely represents the conditions found on

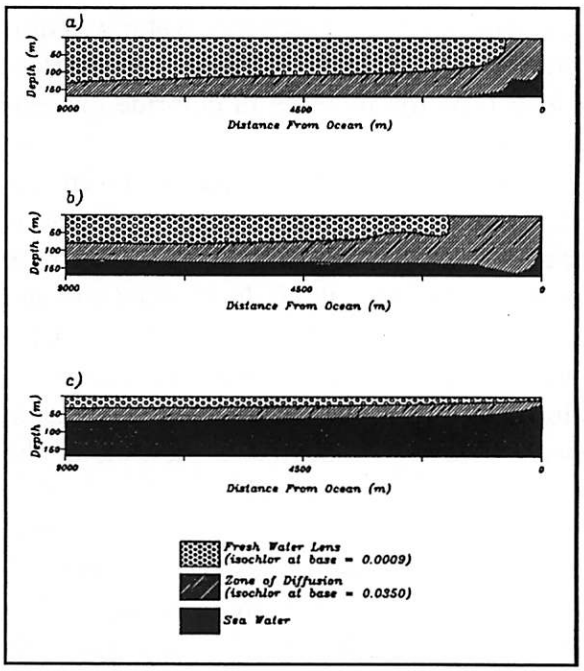

Figure 7. Model results simulating a) homgenous domain, b) Lucayan Limestone and pre-Lucayan, and c) Lucayan, pre-Lucayan, and a paleosol.

Andros Island. This gave an indication that paleosols may be important in understanding fresh water lens thickness, as explored further below.

As a side note, recharge between 15% and 35% of precipitation maintained the fresh water lens with only minor changes in thickness. Small changes in topography did not impact the lens thickness. Only models representing low permeability paleosols resulted in a lens as thin as conceptualized in Figure 3.

After this initial phase, an opportunity arose to conduct pumping tests in two boreholes within the study area, detailed by Bukowski (1996). The results gave transmissivity values of 1.0 x 10^{-1} and 1.6 x 10^{+1} cm^2/s (geometric mean = 4.4 x 10^{0} cm^2/s) with horizontal permeability of 3.8 x 10^{-8} and 7.7 x 10^{-8} cm^2 and vertical permeability of 1.1 x 10^{+4} and 2.2 x 10^{+4} cm^2 giving anisotropy ratios on the order of 3.0 x 10^{+3}. During the pumping tests, water originating above a paleosol at 4 m depth was observed

cascading in the well, resulting in an apparent leaky aquifer effect. Discharge water was also being derived as a result of upward vertical flow evidenced by the increase in chloride concentration with time.

The results of the pumping test were utilized to refine the model grid and parameters. The grid was changed to include the 0.5 m thick paleosol observed in the field at 4 m depth and the 2 m paleosol found at 10-12 m depth. A 1.8 m head change from mid-island to the ocean was included to match the results of a water table elevation survey conducted at the time of the pumping test (Bukowski, 1996).

In the upper 12 m of the grid, horizontal permeability was assigned as 10^{-8} cm^2 and vertical permeability as 10^{-4} cm^2. Paleosols were assigned permeability values from previous models of 10^{-16} cm^2. The 12-40 m portion of the model was assigned an isotropic value of 10^{-4} cm^2. The permeability of the lower part of the model (40 - 170 m) was assigned 10^{-3} cm^2, so that permeability increased with depth. This simulation is shown in Figure 8a. The slight fingering instability is likely a numerical instability due to our Courant and Peclet numbers slightly exceeding unity (Schincariol et al., 1994).

As the anisotropy ratio in the upper 12 m is reduced to 1000 and 100 (Figures 8b and c), the instability is essentially removed from the simulations. The lens thickness from these model runs is approximately 10 m and are the closest to our conceptual model in Figure 3. The result is the same when using the harmonic mean of the layered permeability in the upper 40 m, because the harmonic mean is largely controlled by the low permeability of the paleosols.

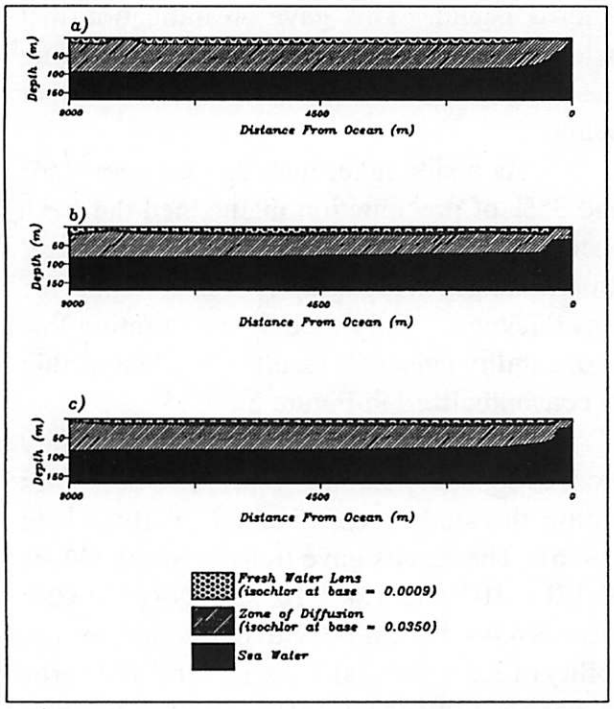

Figure 8. Model results illustrating effects of assigning specific values for vertical and horizontal permeability.

CONCLUSIONS

Results of prior studies by Little et al. (1973), Peach (1991), when combined, lead to a conceptual model where the fresh water lens thickness on Andros Island is on the order of 15 m thick in the center of the island and thins toward the ocean. This is considerably thinner than the Ghyben-Herzberg theoretical lens.

Numerical simulation of the aquifer on Andros Island in this study has been used as an interpretive method for gaining insight into the factors which control the thickness of the fresh

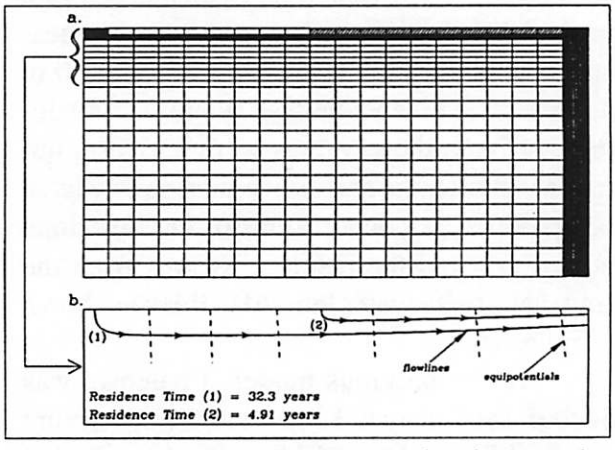

Figure 9. a. shaded cells in grid indicating location of cells from which velocities were taken for residence time calculations; b. expanded view with flow paths

water lens. Neither topographic nor recharge variations in the models resulted in appreciable change in lens thickness. Only simulations which represented discrete intervals of low permeability paleosol horizons at 4 and 10 m gave a lens thickness comparable to the conceptual model.

Within the thin lens, it is interesting to consider ground water residence time and the magnitudes of the velocity vector computed for two flowpaths were examined. The velocity vectors are not strictly connectable as flowlines. However, we took vectors corresponding very closely to the two flow lines shown in Figure 9. Along flowpath 1, approximately 32.3 years elapse between recharge at the mid-island and discharge 9.0 km away at the ocean. Similarly, water recharging the aquifer at a location 4.5 km inland and traveling along flowpath 2 reaches the ocean in 4.9 years.

Like Andros, the fresh water lens on other islands including New Providence and Great Exuma does not follow the Ghyben-Herzberg theory (Cant and Weech, 1986; Wallis et al., 1992; Vacher and Wallis, 1992). Paleosols also exist at similar elevations on these other Bahamian Islands (Beach and Ginsburg, 1980; Shinn and Lidz, 1988; Peach, 1991; Aurell et al., 1995; Boardman et al., 1995; Kenter et al., 1995; Hall, 1996, personal communication) and likely control the generally thin fresh water lenses found throughout the Bahamas.

REFERENCES

Anderson, M. P. and Woessner, W. W., 1992, Applied groundwater modeling, simulation of flow and advective transport: San Diego, Academic Press, 381 p.

Aurell, M., McNeill, D. F., Guyomard, T., and Kindler, P., 1995, Pleistocene shallowing-upward sequences in New Providence, Bahamas: Signature of high-frequency sea-level fluctuations in shallow carbonate platforms: Journal of Sedimentary Research, v. B65, no. 1, p. 170-182.

Beach, D. K. and Ginsburg, R. N.,1980, Facies succession of Pliocene-Pleistocene carbonates, northwestern Great Bahama Bank: The American Association of Petroleum Geologists Bulletin, v. 64, no. 10, p. 1634-1642.

Boardman, M. R., and Carney, C., 1997, Influence of sea level on the origin and Diagenesis of the shallow aquifer of Andros Island, Bahamas: *in* Proceedings, Eighth Symposium on the Geology of the Bahamas, Bahamian Field Station, San Sal vador, Bahamas, p. 13-32.

Boardman, M. R., McCartney, R. F., and Eaton, M. R., 1995, Bahamian paleosols: Origin, relation to paleoclimate, and stratigraphic significance, *in* Terrestrial and shallow marine geology of the Bahamas and Bermuda, Boulder, Colorado. Geological Society of America Special Paper 300, p. 33-47.

Boardman, M. R., Troksa, M. R., and Carney, C., 1992, Variability of lithologic characteristics of a Pleistocene ooid sand shoal Andros Island Bahamas links to the past, *in* Proceedings, Sixth Symposium on the Geology of the Bahamas, Bahamian Field Station, San Salvador, Bahamas, p. 1-15.

Bukowski, J. M, 1996, Modeling the Fresh Water - Salt Water Interface in the Pleistocene Aquifer on Andros Island, Bahamas [M.S. Thesis]: Wright State University, 90 p.

Cant, R. V. and Weech, P. S., 1986, A review of the factors affecting the development of Ghyben-Hertzberg lenses in the Bahamas: Journal of Hydrology, v. 84, p. 333-

343.

Carney C. and Boardman, M. R., 1993, Trends of sedimentary microfabric of ooid tidal channels and deltas in Frontiers in Sedimentary Geology: Carbonate Microfabrics: New York, Springer Verlag, p. 29-39.

Fetter, C. W., 1972, Position of the saline water interface beneath oceanic islands: Water Resources Research, v. 8, no. 5, p. 1307-1315.

Griggs, J. E., 1989, Numerical simulation of groundwater development schemes for the Laura area of Majuro Atoll, Marshall Islands [PhD Thesis]: Univ. of Hawaii, 203 p.

Griggs, J. E. and Peterson, F. L., 1989, Ground water flow and development alternatives: A numerical simulation of Laura, Majuro Atoll, Marshall Islands: Technical Report 183, University of Hawaii at Manoa Water Resources Center, Honolulu, 91 p.

Hall, E., 1996, Personal Communication: Water and Sewerage Corporation, Nassau, Bahamas.

Herman, M. E., and Wheatcraft, S. W., 1984, Groundwater dynamics investigation of Enjebi Island, Enewetak Atoll: An interpretive computer model simulation. *in* Finite Elements in Water Resources, New York, Springer-Verlag p. 133-142.

Hogan, P., 1988, Modeling of freshwater-seawater interaction on Enjebi Island, Enewetak Atoll [M.S. Thesis]: San Jose State University, 75 p.

Kenter, J. A. M., Kievman, C. M., and Ginsburg, R. N., 1995, Sedimentary evidences of Neogene sea levels on the leeward margin of Great Bahama Bank: Society of Economic Paleontologists and Mineralogists, Congress programs and abstracts, v. 1, p. 74-75.

Little, B. G., Buckley, D. K., Jefferiss, A., Stark, J., and Young, R. N., 1973, Land resources of the commonwealth of the Bahamas, volume 4a Andros Island: Land Resources Division, Tolworth Tower, Surrey, England, KT6 7DY. p. 40-110.

Lloyd, J. W., 1991, A study of saline groundwater responses to abstraction from trenches in the Bahamas: United Nations Development Programme Department of Technical Co-Operation for Development, Project BHA/86/004/A/01/01. 16 p.

Oberdorfer, J. A., Hogan, P. J., and Bukkemeier, R. W., 1990, Atoll island hydrogeology: flow and freshwater occurrence in a tidally dominated system: Journal of Hydrology. v. 120, p. 327-340.

Peach, D. W., 1991, Hydrogeological investigations of New Providence and North Andros: United Nations Development Programme Department of Technical Cooperation for Development, Project BHA/86/004.

Schincariol, R. A., Schwartz, F. W., and Mendoza, C. A., 1994, On the generation of instabilities in variable density flow: Water Resources Research, v. 30, no. 4, p. 913-927.

Sealey, N. E., 1994, Bahamian Landscapes, An introduction to the geography of the Bahamas: Nassau, Bahamas, Media Publishing, 128 p.

Shinn, E. A. and Lidz, B. H., 1988, Blackened

limestone pebbles: fire at subaerial unconformities: *in* Paleokarst, New York, Springer Verlag, p. 117-131.

Thurman, H., 1991, Introductory Oceanography, Sixth Edition: Columbus, Merril Publishing, 526 p.

Underwood, M. R., 1990, Atoll island hydrogeology: Conceptual and numerical model, [PhD Thesis]: University of Hawaii, 205 p.

Underwood, M. R., Peterson, F. L., and Voss, C. I., 1992, Groundwater lens dynamics of atoll islands: Water Resources Research, v. 28, no. 11, p. 2889-2902.

Vacher, H. L, and Wallis, T. N., 1992, Comparative hydrogeology of fresh-water lenses of Bermuda and Great Exuma Island, Bahamas: Ground Water, v. 30, no. 1, p. 15- 20.

Voss, C. I., 1984, A finite-element simulation model for saturated-unsaturated, fluid-density-dependent ground-water flow with energy transport or chemically-reactive single-species solute transport: USGS Water-Resources Investigations Report 84-4369, 409 p.

Wallis, T. N., Vacher, H. L., and Stewart, M. T., 1992, Hydrogeology of fresh water lens beneath a Holocene strandplain, Great Exuma, Bahamas: Journal of Hydrology, v. 125, p. 93-109.

Weech, P., 1995, Personal Communication: Water and Sewerage Corporation, Nassau, Bahamas.

Wicks, C. M. and Herman, J. S., 1995, The effect of zones of high porosity and permeability on the configuration of the saline-freshwater mixing zone: Ground Water, v. 33, no. 5, p. 733-740.

Wolfe, P. J., Carney, C., and Boardman, M. R., 1995, Blue hole and beachrock geophysics, in Proceedings, Symposium on the Application of Geophysics to Engineering and Environmental Problems, p. 889-892.